

One-Step Synthesis of Silica@Resorcinol-Formaldehyde Nanospheres and their Application for the Fabrication of Functional Polymer and Carbon Capsules

Antonio B. Fuertes*, Patricia Valle-Vigón and Marta Sevilla

Core@shell spheres made up of a thin layer of resorcinol–formaldehyde enveloping a silica core were prepared by means of a one-step method under Stöber conditions. These spheres are used as a platform for the synthesis of carbon or polymeric capsules, and functionalized nanocomposites.

The synthesis of silica, carbon or polymer nanospheres and capsules has attracted widespread interest because of their potential applications in the fields of drug delivery, catalysis, photonic crystals, biodiagnostic or energy storage.^[1] Special attention has been paid to colloidal silica nanospheres of uniform size. These particles are commonly produced by the hydrolysis and condensation of silicon alkoxides (i. e. tetraethyl orthosilicate, TEOS) in a water-ethanol mixture in the presence of ammonia as catalyst (Stöber method).^[2] Recently, this simple procedure has been successfully extended to the fabrication of monodisperse polymeric nanospheres of resorcinol–formaldehyde (RF).^[3] The numerous similarities between the reaction mechanisms in the synthesis of colloidal silica and resorcinol-formaldehyde, both of which are catalysed by ammonia, foreshadowed the success of this strategy.^[4] However, it is worth mentioning one important difference between both processes; i. e. they occur at very different reaction rates. Indeed, whereas the synthesis of Stöber silica particles takes only ~ 1 hour (30 °C), the formation of RF nanospheres occurs slowly and requires long reaction times (~ 24 h at 30 °C).^[3a] The fact that both processes take place under similar reaction conditions (i. e. reaction medium, temperature and catalyst) but over different time scales immediately suggests that the one-step synthesis of silica-RF nanocomposites is feasible with a rationally designed synthesis scheme. In order to prove this hypothesis, we

[*] Prof. A. B. Fuertes, P. Valle-Vigón, Dr. M. Sevilla
Instituto Nacional del Carbón (CSIC), P. O. Box 73, 33080-Oviedo (Spain)
Fax: (+34) 985-297662
E-mail: abefu@incar.csic.es

investigate the synthesis of silica-RF nanocomposites under Stöber conditions: a) ethanol/water mixtures as the reaction medium and b) ammonia as catalyst and structuring-direct agent. In this way, core@shell nanospheres made up of a silica core coated with a thin polymeric RF layer (silica@RF) were successfully synthesized. To the best of our knowledge, this is first time that a one-step synthesis of highly monodisperse silica-polymer nanospheres with a core@shell structure has been reported.

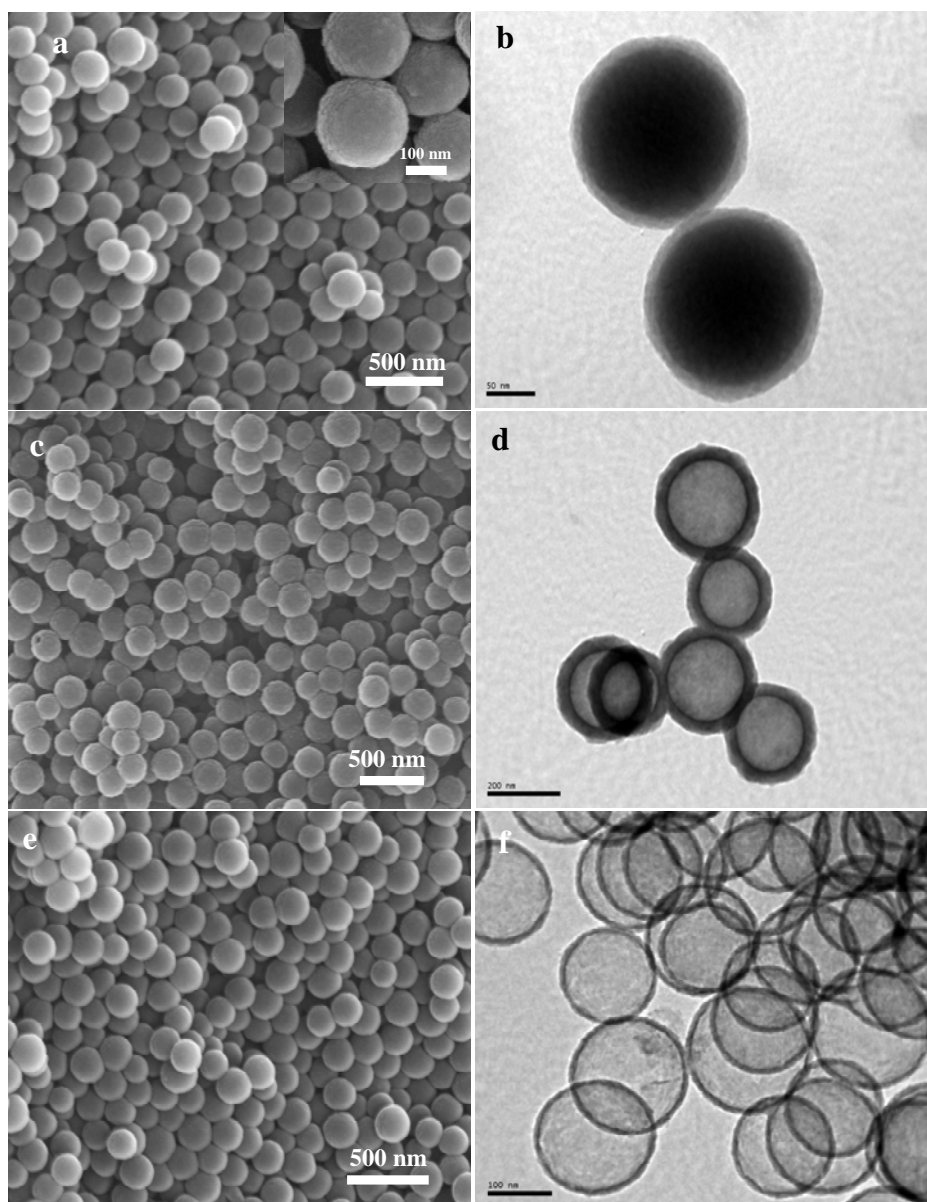
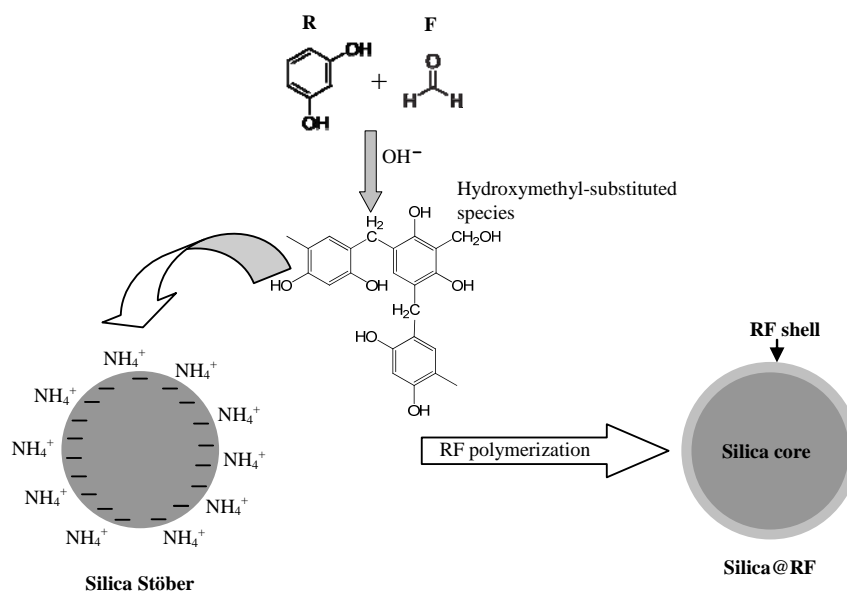


Figure 1. SEM (a, c, e) and TEM (b, d, f) images of silica@RF nanospheres (a, b), resorcinol-formaldehyde capsules (c, d) and carbon capsules (e, f). ($E/W=2$, $C_{TEOS}=0.16 \text{ mol}\cdot\text{L}^{-1}$).

Under Stöber reaction conditions, it can be assumed that the polymerization reactions of silica and resorcinol-formaldehyde occur consecutively. Firstly, the formation of the silica nanospheres takes place. This process depends heavily on the hydrophilic-hydrophobic balance of the reaction medium, which is determined by the ethanol/water (E/W) volumetric ratio. In the classical Stöber method a high (E/W) ratio of ~ 7 is commonly used,^[5] but lower (E/W) ratios are also effective. In this regard, we found that silica nanospheres can be successfully fabricated at an (E/W) ratio as low as ~ 2 , but not below this limit. On other hand, when the synthesis of silica-RF is carried out at resorcinol (R) concentrations of > 0.06 M, the resulting silica-RF composite is made up of large agglomerates of welded nanoparticles (see Figure S1a). Taking into account all of these restrictions, we selected the most appropriate synthesis parameters, which are listed in Table S1 (in Supporting Information) together with the typical values used in the synthesis of Stöber silica and RF nanospheres. The material produced under these conditions has a brown-reddish colour and it is made up of uniform spherical nanoparticles with a core@shell structure consisting of a silica core and a polymeric shell. The SEM images shown in Figure 1a (and Supporting Information, Figure S3a and S4a) reveal that these silica@RF nanospheres have a uniform size (*e. g.* 220 ± 18 nm at $C_{\text{TEOS}} = 0.16$ M, E/W=2) and a slightly rough surface (see inset in Figure 1a). The core@shell structure of these particles is clearly illustrated by the TEM image in Figure 1b and also by the silica nanospheres obtained after the calcination of the composite (see Figure S1b). The thickness of the RF shell enveloping the silica nanospheres is ~ 20 -30 nm, as deduced from the high-magnification TEM images of the RF capsules obtained after the removal of the silica (see Figure S2).

The diameter of the silica@RF nanospheres can be adjusted by varying the concentration of the silica precursor (TEOS) and the (E/W) ratio used in the synthesis. As the concentration of TEOS varies from 0.06 M to 0.36 M (E/W=2), the diameter of the nanospheres gradually rises from 150 ± 16 nm to 300 ± 21 nm (see Figure S3b). Moreover, by increasing the (E/W) ratio from 2 to 7 the diameter of the silica@RF nanospheres can be increased systematically from 232 ± 22 nm to 489 ± 33 nm (see Figure S4b) ($C_{\text{TEOS}} = 0.2 \text{ mol}\cdot\text{L}^{-1}$). The composition of the silica@RF nanospheres can also be regulated by modifying the concentration of TEOS used in the synthesis. Indeed, thermogravimetric analysis (data not shown) reveals that the RF/silica weight ratio

uniformly increases from 0.3 to 1 as the TEOS concentration decreases from 0.36 mol·L⁻¹ to 0.06 mol·L⁻¹ (E/W=2).



Scheme 1. Synthesis scheme of the formation of silica@RF nanospheres.

Scheme 1 illustrates the mechanism proposed for the formation of silica@RF nanospheres. In a first step, Stöber silica nanospheres are rapidly generated. NH₄⁺ ions cover the outer surface of the silica nanoparticles (negatively charged) thereby preventing their aggregation and allowing the formation of a stable colloidal suspension. Parallel to the formation of the silica particles there occurs a slower reaction between the resorcinol and formaldehyde catalysed by the OH⁻ ions. As a result of this reaction, hydroxymethyl-substituted species are formed. According to the hypothesis of Liu et al.^[3a] in relation to the formation of RF nanospheres, a large number of hydroxymethyl substituted species will diffuse to the surface of the silica nanoparticles due to the electrostatic interaction with the NH₄⁺ ions located there. Condensation between these species will occur within the nanospace surrounding the silica particles resulting in the formation of an RF polymeric layer around the silica nanospheres.

The core@shell structure of the silica@RF nanospheres immediately suggests an easy route towards the fabrication of polymer (resorcinol-formaldehyde) and carbon capsules as illustrated in Scheme S1 (see SI). The hollow nanoparticles have attracted widespread attention because of their capacity for storing substances inside their internal cavities, a function which is relevant for a variety of applications (e. g. high-

performance catalyst supports, drug delivery systems, lithium-ion batteries or carriers for the adsorption and immobilization of biomolecules).^[1a, 6] The synthesis procedures for carbon or polymeric capsules are complex and they normally entail multiple steps and a previously synthesized hard template.^[7] The development of simpler synthetic routes towards the fabrication of uniform polymer and carbon capsules is still an important challenge and significant efforts are being made to accomplish this objective.^[8] In this regard, the use of silica@RF nanospheres clearly simplifies the fabrication process of both types of capsules. Indeed, we show that polymeric capsules of resorcinol–formaldehyde can be generated by dissolving the silica core of the silica@RF spheres. They are illustrated by the SEM and TEM images in Fig. 1c and d (and Fig. S2, ESI).

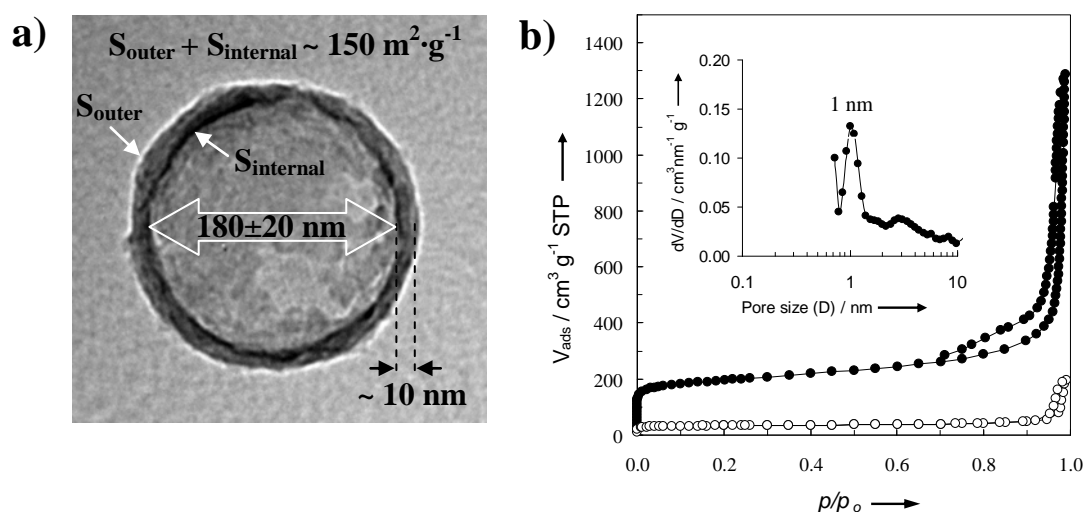


Figure 2. (a) Structure of a carbon capsule illustrated by means of a TEM image and (b) nitrogen sorption isotherms for silica@carbon composites (open symbols) and carbon capsules (black symbols) (Inset: pore size distribution for the carbon capsules). ($E/W=2$, $C_{\text{TEOS}}=0.16 \text{ mol}\cdot\text{L}^{-1}$)

To produce carbon capsules, the silica@RF nanoparticles were heat-treated in nitrogen to convert the RF polymeric layer into carbon (see Figure S5a for the weight changes during the carbonization step). Subsequently, the carbonized product formed by silica@carbon nanospheres (see Figure S5b) was washed with hydrofluoric acid to dissolve the silica core. The carbon capsules obtained are monodisperse as can be seen from the SEM images shown in Figures 1e (and Supporting Information, Figures S3a

and S4a) and their diameters can uniformly vary over a wide range from ~ 130 nm to ~ 450 nm by modifying the TEOS concentration or the (E/W) ratio used for the synthesis of the silica@RF composites (see Figures S3b and S4b). The hollow structure of these nanoparticles is illustrated by the TEM images shown in Figures 1f and Figure S6. The particles consist of a uniform carbon layer ~ 10 nm thick that envelops a large void of diameter 180 ± 20 nm (E/W=2, $C_{\text{TEOS}}=0.16$ M) as illustrated in Figure 2a. Nitrogen physisorption measurements reveal that these hollow carbon particles have a high BET surface area of $720 \text{ m}^2 \cdot \text{g}^{-1}$ (Figure 2b). Importantly, the carbon shell contains confined micropores, the micropore volume being $0.2 \text{ cm}^3 \cdot \text{g}^{-1}$. These micropores have a size of around 1 nm (Figure 2b inset). Most of the BET surface area corresponds to these micropores ($\sim 550 \text{ m}^2 \cdot \text{g}^{-1}$ as deduced by *t*-plot) the rest being the sum of the outer and internal surfaces ($\sim 150 \text{ m}^2 \cdot \text{g}^{-1}$) of the capsule, as illustrated in Figure 2a. These results show that the carbon shell is permeable, which is important since it means that these hollow particles can be used as nanocontainers. These hollow carbon nanospheres can also be employed as supports onto which inorganic nanoparticles can be deposited or as templates for producing inorganic hollow nanocapsules. Both types of materials have great relevance for catalysis and in electrochemical devices (i. e. supercapacitors or lithium-ion batteries).^[6a, 9] In the present study we investigated the preparation of both materials as illustrated in Scheme S1 (see ESI). This strategy was applied to the synthesis of: (a) SnO₂ nanoparticles deposited onto carbon capsules (see Fig. S7, ESI) and (b) highly monodisperse SnO₂ capsules (see Fig. S8, ESI).

The silica@RF nanospheres can easily be post-functionalized to incorporate diverse groups in high density due to the reactive organic functionalities present in the polymer shell. This alternative was analysed by two examples: a) the incorporation of sulphonic acid groups (-SO₃H) *via* sulphonation with concentrated sulphuric acid (silica@RF-SO₃H) and b) the introduction of primary amino groups by silylation of the -OH functionalities using (3-aminopropyl)triethoxysilane (APTES) (silica@RF-NH₂). Figure 3a schematically illustrates the synthesis conditions employed in both cases. Evidence of the incorporation of these functional groups is obtained by comparing the FT-IR spectra of the silica@RF with the post-functionalized samples (Figure 3b). Specifically, the silica@RF-NH₂ nanospheres exhibit a IR band at $\sim 1050 \text{ cm}^{-1}$ due to C-N stretching vibrations of primary aliphatic amines and the silica@RF-SO₃H particles exhibit a sharp peak at 1040 cm^{-1} characteristic of symmetric O=S=O stretching

vibrations, revealing the presence of $-\text{SO}_3\text{H}$ groups.^[10] Elemental analysis confirmed the presence of sulphur and nitrogen in the silica@RF- SO_3H and silica@RF- NH_2 samples in quantities of 0.7 wt % S and 2.4 wt % N respectively, the surface densities being $\sim 15 \mu\text{mol S}\cdot\text{m}^{-2}$ and $\sim 110 \mu\text{mol N}\cdot\text{m}^{-2}$. It must be emphasized that our approach is very flexible and can be applied to incorporate a variety of functional groups following the well-described procedures in the literature.^[11]

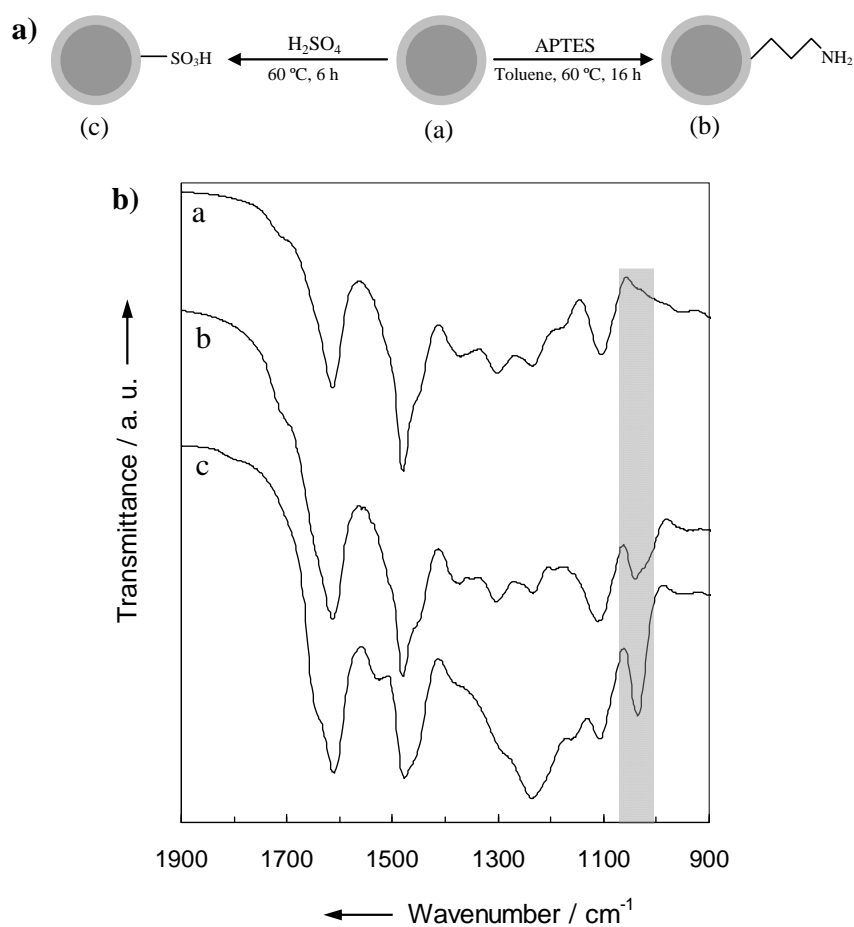


Figure 3. (a) Synthesis scheme employed for the functionalization of the silica@RF nanospheres and (b) FT-IR spectra of: (a) silica@RF, (b) silica@RF-NH₂ and (c) silica@RF-SO₃H nanospheres.

In summary, we have developed a new, versatile and facile one-step methodology to produce uniform silica@RF nanospheres with a core@shell structure. To our knowledge, this is the first time a one-step synthesis of uniform silica@polymer nanospheres has been achieved. The success of the strategy is based on combining the

synthesis processes of silica and resorcinol-formaldehyde under Stöber conditions (i. e. an ethanol-water medium and the presence of ammonia). The diameter of the silica@RF nanospheres can be tuned from 150 nm to 500 nm by modifying the ethanol/water ratio or the concentration of the silicon alkoxide. The silica@RF nanospheres constitute an excellent platform for the fabrication of uniform hollow particles of carbon or resorcinol-formaldehyde. The diameter of these capsules can be finely tuned over a wide range (130-450 nm) depending on the silica@RF sample used as precursor. The functionalization of such core@shell nanospheres was demonstrated by incorporating sulphonic and amino groups to the resorcinol-formaldehyde shell. The variety of advanced materials here presented has a considerable interest due to their possible application in catalysis, drug delivery, electrochemistry, selective adsorption and nanocasting.

This work was supported by Spanish MICINN (Project CQT2011-24776). M.S. and P.V-V. acknowledge the Ramon y Cajal and JAE-Predoc contracts respectively

References

- [1] a) X. W. Lou, L. A. Archer, Z. Yang, *Adv. Mater.* **2008**, *20*, 3987; b) M. Liong, J. Lu, M. Kovoichich, T. Xia, S. G. Ruehm, A. E. Nel, F. Tamanoi, J. I. Zink, *ACS Nano*, *2008*, *2*, 889; c) T. L. Kelly, M. O. Wolf, *Chem. Soc. Rev.* **2010**, *39*, 1526; c) H. Goessmann, C. Feldmann, *Angew. Chem. Int. Ed.* **2010**, *49*, 1362.
- [2] a) W. Stöber, A. Fink, E. Bohn, *J. Colloid Interface Sci.* **1968**, *26*, 62; b) L. Jelinek, P. Dong, C. Rojas-Pazos, H. Talbi, E. Kovats, *Langmuir* **1992**, *8*, 2152; c) D. L. Green, J.S. Lin, Y.-F. Lam, M. Z.-C. Hu, D. W. Schaefer, M.T. Harris, *J. Colloid Interface Sci.* **2003**, *266*, 346.
- [3] a) J. Liu, S. Z. Qiao, H. Liu, J. Chen, A. Orpe, D. Y Zhao, G. Q. (Max) Lu, *Angew. Chem. Int. Ed.* **2011**, *50*, 5947; b) A.-H. Lu, G.-P. Hao, Q. Sun, *Angew. Chem. Int. Ed.* **2011**, *50*, 9023.
- [4] a) C. J. Brinker, *J. Non-Cryst. Solids* **1988**, *100*, 31; b) A. M. El-Khatat, S. A. Al-Muhtaseb, *Adv. Mater.* **2011**, *23*, 2887.
- [5] G. Büchel, K. K. Unger, A. Matsumoto, K. Tsutsumi, *Adv. Mater.* **1998**, *10*, 1036.

- [6] a) J. Hu, M. Chen, X. Fang, L. Wu, *Chem. Soc. Rev.* **2011**, *40*, 5472; b) Z. Lei, J. Zhang, X. S. Zhao, *J. Mater. Chem.*, **2012**, *22*, 153; d) X. Lai, J. E. Halpert, D. Wang, *Energy Environ. Sci.*, **2012**, *5*, 5604
- [7] a) S. B. Yoon, K. Sohn, J. Y. Kim, C.-H. Shin, J.-S. Yu, T. Hyeon, *Adv. Mater.* **2002**, *14*, 19; b) M. Kim, K. Sohn, H. B. Na, T. Hyeon, *Nano Lett.*, **2002**, *2*, 1383; c) G. Liu, H. Zhang, X. Yang, Y. Wang, *Polymer* **2007**, *48*, 5896; d) Y. Wang, V. Bansal, A. N. Zelikin, F. Caruso, *Nano Lett.*, **2008**, *8*, 1741.
- [8] a) S. H. Im, U. Jeong, Y. Xia, *Nature Mater.*, **2005**, *4*, 671; b) D. Kim, E. Kim, J. Kim, K. M. Park, K. Baek, M. Jung, Y. H. Ko, W. Sung, H. S. Kim, J. H. Suh, C. G. Park, O. S. Na, D. Lee, K. E. Lee, S. S. Han, K. Kim, *Angew. Chem. Int. Ed.* **2007**, *46*, 3471; c) P. Valle-Vigón, M. Sevilla, A. B. Fuertes, *Chem. Mater.* **2010**, *22*, 2526; d) A.-H. Lu, W.-C. Li, G.-P. Hao, B. Spliethoff, H.-J. Bongard, B. B. Schaack, F. Schüth, *Angew. Chem. Int. Ed.* **2010**, *49*, 1615.
- [9] a) C. Liu, F. Li, L.-P. Ma, H.-M. Cheng, *Adv. Mater.* **2010**, *22*, E28; b) D. S. Su, R. Schlögl, *ChemSusChem* **2010**, *3*, 136; c) Z. Wang, L. Zhou, X. W. Lou, *Adv. Mater.* **2012**, DOI: 10.1002/adma.201200469.
- [10] G. Socrates, *Infrared and Raman Characteristic Group Frequencies*, 3rd ed., Wiley, New York, **2005**.
- [11] a) A. Kirschning, H. Monenschein, R. Wittenberg, *Angew. Chem. Int. Ed.* **2001**, *40*, 650; b) F. Hoffmann, M. Cornelius, J. Morell, M. Fröba, *Angew. Chem. Int. Ed.* **2006**, *45*, 3216.